[SSC24-V-06]

Debris Detection Using Star Tracker Concept Verification

Laila Kazemi, Alexander Vandenberghe, Mikel Samson, Bram Vandoren, Tjorven Delabie
arcsec
Blijde Inkomststraat 22, 3000 Leuven, Belgium
Phone: +32 498 81 73 70; Mail: firstname@arcsecspace.com

ABSTRACT

This paper demonstrates the concept of space debris detection using star trackers. Arcsec's Sagitta star tracker is an optical sensor designed to determine spacecraft attitude based on captured star images. The Sagitta star tracker processes these images to extract bright regions, which are then compared to an on-board star database. This functionality can also be extended to detect and track space debris passing through the sensor's field of view. Typical star trackers discard any bright objects that are not matched to their star database. With addition of Debris Detection Using Star Trackers (DeDUST) algorithm, Sagitta can isolate these observations. Star tracker observations of space debris can be used for orbit determination, allowing for conjunction analysis or intelligence gathering. The Sagitta star tracker can concurrently perform attitude determination at 10 Hz while running the DeDUST algorithm to obtain precise angular measurements of objects passing through the field of view. These observations are later downlinked for orbit determination. Implementing space debris detection and tracking on star trackers, which are present on the majority of satellites, allows for a vast increase in space situational awareness (SSA) without the need to launch dedicated space-based sensors. The concept is proven to work on a Sagitta star tracker mounted on the Mercator observatory in La Palma, by observing space objects, determining their orbits, and matching them to known object catalogs.

Introduction

According to ESA's Space Environment Report, over 30,000 objects are measuring 10 cm or larger in the LEO and GEO environments, along with more than one million smaller objects.[1] Emerging guidelines from global space governance bodies are now requiring spacecraft operators to contribute to the SSA domain and clean space initiatives. Space debris is congesting Earth's orbits. Debris elements – even very small ones – have the potential to destroy satellites or manned vehicles.

Concurrently, due to the popularity of constellations, the number of launched spacecraft is growing rapidly, further complicating the situation. There is an urgent need for space traffic management, collision avoidance capabilities, and space debris removal. All these elements require an accurate and comprehensive mapping of space debris. Currently, significant gaps exist in the available space debris data, especially regarding elements smaller than 10 cm. There are hundreds of thousands of such elements in orbit, each with the potential to severely damage or even destroy spacecraft.

The available ground-based sensor networks have limited spatial resolution and gaps in certain geographical areas, such as the Southern Hemisphere. Additionally, there is very limited statistical information on how congested certain orbits are. To obtain this critical information, a space-based network with a high number of sensors is needed, as it requires numerous observations. The cost of space debris data, excluding information freely provided by governments, is significant, reducing the margin for providing downstream services. It is also counter intuitive to launch dedicated space debris detection missions to tackle the problem of space traffic.

Opportunity

A star tracker is an optical sensor onboard a satellite that captures and processes star images to determine the spacecraft's orientation. The increasing computational capabilities of star tracker microcontrollers, coupled with their integration into the majority of spacecraft buses, present an opportunity to incorporate additional functionality. Since star trackers are optimized to detect bright objects, they are also well-suited for detecting space debris that reflects light. As opposed to other space-based systems, no dedicated satellites with dedicated payloads are needed. The debris is detected with the same sensor that determines the spacecraft attitude, allowing to calculate the debris orbit with high ac-

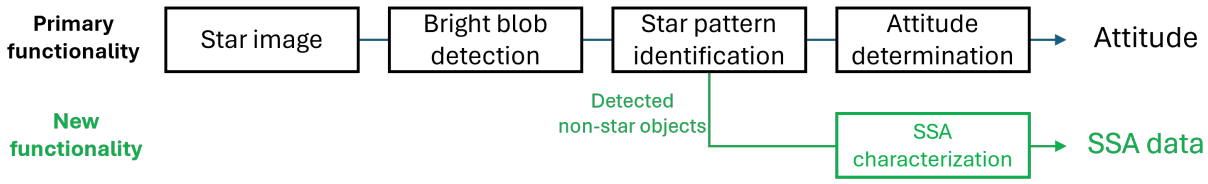

Figure 1: Workflow of the star tracker algorithm with added functionality.

curacy. Figure 1 illustrates workflow of star tracker algorithms with added functionality of debris detection.

The proposed solution is extremely cost-effective as there is no dedicated hardware or mission cost. The cost is very limited to slight increased power consumption and extra downlink budget (Only in the range of kBs). Figure 2 presents the position of the proposed solution in comparison to current solutions for detectable size of space debris and its cost.

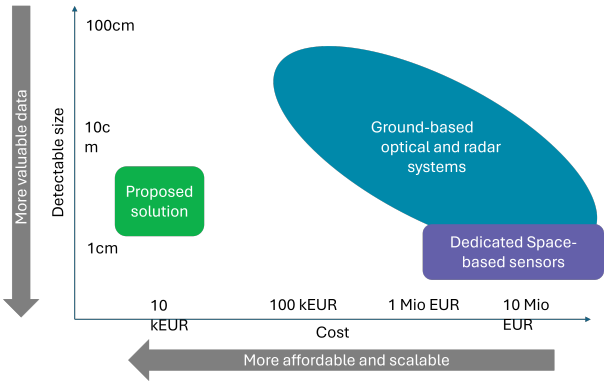

Figure 2: Solution cost and detectable debris size trade-off for current and the proposed solution.

Approach

Typically, star trackers discard non-star data, but the proposed algorithm processes non-star signals to identify and track potential space debris. After matching the detected objects with the onboard star catalog, the unmatched objects are tracked via an intermediate database to identify potential debris candidates.

The performance of this tracking filter can be enhanced by adjusting its parameters using available blob information, such as the brightness or shape of the blob. The weighting matrix of the filter can be adjusted to improve the position estimates of stars and debris. Furthermore, the algorithm estimates the uncertainty of the blob positions, which is propagated for processing debris measurements to obtain their orbit parameters and integrate the data with existing space debris databases.

The intermediate dataset tracks potential debris candidates based on their brightness, position, and velocity within the image frame. Debris candidates characterized and tracked in multiple image frames are eventually transferred to the main debris dataset and orbital parameter estimator. To simulate and test this functionality, high-fidelity star tracker images, including space debris, are generated using MATLAB. The proposed algorithm is computationally efficient and can run in real-time on the Sagitta star tracker in parallel with attitude estimation algorithms at a typical rate of 10 Hz. A series of night sky tests were conducted to test the onboard implemented algorithm, successfully detecting and characterizing several known objects.

The orbit determination process combines consecutive observations of the same object to build an evolving SSA catalog. The main error sources in the estimation process stem from position and time knowledge in the star tracker. These errors can be partially mitigated through tight integration with an onboard GNSS receiver. A study of mission profiles indicates that Sagitta can track upwards of 1,000 debris elements per day. Using DeDUST data, a comprehensive space debris database can be formed, and scalable with the number of Sagitta star trackers operating on orbit.

Literature Review

This section reviews current literature and technology on space-based debris detection by optical sensors and in particular star trackers. The proof of concept studies have been carried out on simulated images[2][3][4] and real sky images[5] , proving the potential to detect and characterize debris and artificial objects. Spiller et al.[2] developed high fidelity simulator for star trackers including space debris observations and validated this simulation. They characterized star tracker measurement based on the location and motion of the image frame. They also discussed the challenges of implementing the pro-

posed solution on-board the star tracker, however, the on-board implementation was not tested.

Liu et al.[3] explore the advantages of simultaneous measurements from multi-star tracker systems. This work explores multi-sensor data fusion of debris measurements. Denver et al.[5] investigated the characterization of debris detection performance on the µASC star tracker from DTU (Technical University of Denmark). They implemented similar techniques used by the NASA JUNO mission detecting and tracking natural objects in orbit around Jupiter. Zamani et al.[4] develop vision-based detection, tracking, and classification algorithms to address extracting space debris information from optical sensors. They worked on optimizing algorithms for performance as well as computational effort.

Paper Outline

The remainder of this paper is structured into five main sections. It begins with an introduction to the baseline sensor, detailing its key properties relevant to this study. This section also addresses the processing noise associated with star centroid measurements.

Next, the debris detection and tracking framework is presented, focusing on the implementation of Kalman filtering for star tracker centroids and the categorization of detected bright objects into stars and debris. The subsequent section elaborates on the orbit determination procedure based on star tracker debris measurements, describing the main models employed and the estimation approach utilized.

Following this, the experimental setup is detailed, including the environment, procedures, and data analysis methods. The results from the night sky observations are then discussed, with the detected object characterized and matched to a known satellite. Finally, the paper concludes by summarizing key findings, discussing implications, suggesting future research directions, and providing closing remarks.

Sensor Models

The sensor model implemented for debris simulation and testing the characterization algorithms is based on arcsec's Sagitta star tracker. The Sagitta star tracker is a compact and high-accuracy star tracker. The star tracker is a fully autonomous unit and has a built-in baffle (see: Figure 3). Table 1 lists the main optical and detector parameters of Sagitta star trackers.

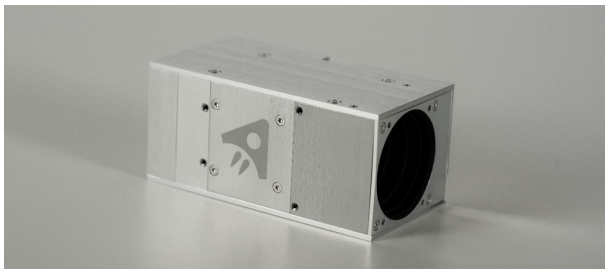

Figure 3: Sagitta star tracker.

Table 1: Sagitta Star Tracker Detector and Optical Parameters

Field of View (FOV)	25.4° Full Cone
Focal Length	25 mm
Lens Diameter	18 mm
Detector Dimensions	2048x2048 pixels
Exposure Time	100 ms
PSF Size	0.8 pixel 1σ
Detection Magnitude Limit	6.2

A pinhole camera ray tracing model is used to place stars and debris on the star tracker images. Figure 4 shows the basic pinhole camera model with Sagitta star tracker frames of reference. Arcsec already carried out an initial study using ground-based observations. The research concluded that space debris detection can be carried out with the same optical parameters (focus, aperture, etc.) and camera settings (integration time, gains, etc.) used during attitude determination. As long as the algorithms can run efficiently enough to be executed in parallel within the required time, there is no issue with carrying out both functionalities at the same time.

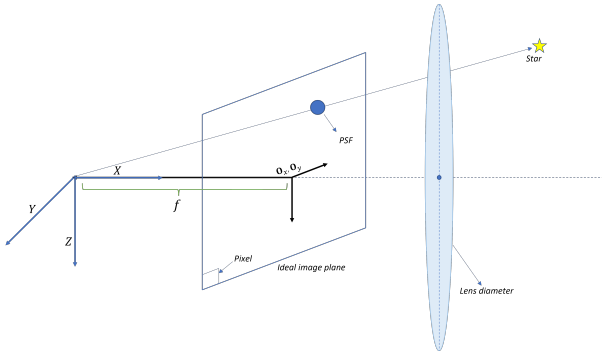

Figure 4: Pinhole camera ray tracing model.

The total photons collected from a star or space debris with a visual magnitude of m is denoted as

I_T and modeled by the equation:

$$I_T = \frac{1}{4}\eta_Q t_e \pi D^2 \phi_0 10^{\frac{-2}{5}m}, \quad (1)$$

Where η_Q is the detector quantum efficiency, t_e is the exposure time, D is the lens diameter and ϕ_0 is the photon flux from a reference star. The pattern the starlight forms where it coincides with the image frame is called the point spread function (PSF), and it is typically modeled as a 2D Gaussian by:

$$I(x,y) = \frac{I_T.G}{2\pi\sigma_x\sigma_y} e^{\left[\frac{(y-C_y)^2+(x-C_x)^2}{2\sigma_x\sigma_y}\right]}, \quad (2)$$

where G convert the detected number of photons I_T to detector count, (σ_x, σ_y) are the Gaussian distribution standard deviation, and (C_x, C_y) are the center of the PSF.

Centroiding Stability

For star and debris detection and tracking, it is important to quantify the star tracker centroiding noise. PSFs with varying visual magnitudes between 0 and 6.2 were simulated 10^3 times, and their centroids were calculated. Delabie et al.[6] proposed a Gaussian centroiding algorithm for star trackers, which is implemented in this work. The tests computed each PSF centroid and their standard deviation. Figure 5 plots the centroid stability as a function of the PSF's visual magnitude. The centroiding error increases with the star's visual magnitude and as the signal-to-noise ratio decreases. This model is used for centroiding process noise in the next section.

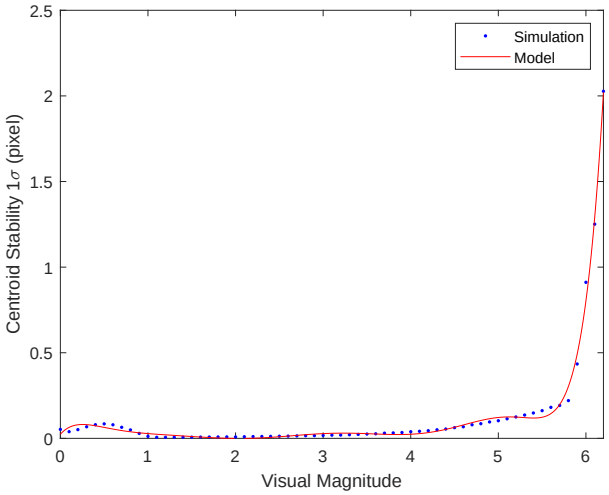

Figure 5: Star centroiding noise.

Sensor Availability

To collect space debris measurements from star trackers continuously, the attitude solution must be available for most of the orbit duration. Several Sagitta star trackers are operational on-orbit. Arcsec performed performance analysis on the on-orbit returned telemetry provided by Sagitta's end users. Figure 6 plots the calibrated quaternion field of the on-orbit telemetry. The eclipse sections are marked in both figures with a dark background. The section during daylight where the Sagitta star tracker loses attitude solution is due to the presence of Earth in the star tracker's field of view. The Sun remains in the opposite hemisphere with respect to the star tracker throughout the entire data set. The Sagitta star tracker provides an attitude solution continuously in the absence of bright celestial objects in its field of view.

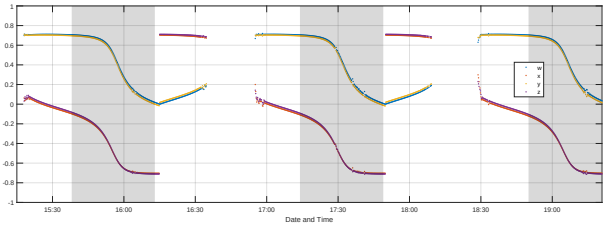

Figure 6: Sagitta star tracker availability.

Sensor Accuracy

The star tracker attitude solution accuracy also impacts space debris measurements. The line-of-sight measurements of debris in the star tracker frame will be rotated into the Earth-centered inertial (ECI) frame by the star tracker attitude solution for the characterization algorithm. The star tracker returned quaternion must be sufficiently accurate to determine the space debris' orbit from the vector measurement in the ECI frame. To estimate the accuracy of the Sagitta star tracker attitude solution, the method proposed by Liebe[7] was used. Figure 7 plots the estimated accuracy of the Sagitta star trackers based on on-orbit returned telemetry. The Sagitta star tracker provides the average centroiding error between the database star and the detected centroid, as well as the total number of stars matched. This centroiding error, combined with the optical characteristics of the sensor, provides an estimate of attitude solution accuracy in the across-boresight and along-boresight directions.

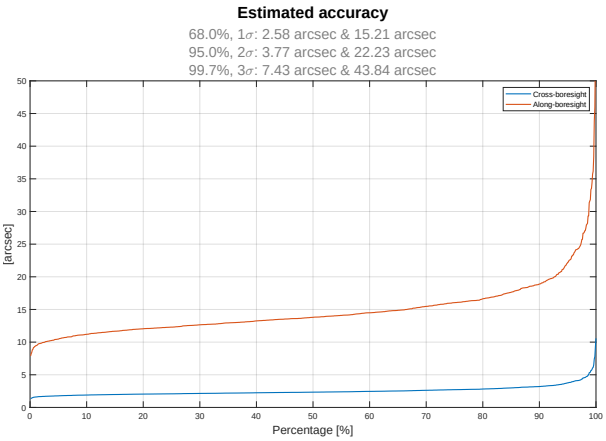

Figure 7: Sagitta star tracker accuracy.

Detection and Tracking Framework

A star tracker is designed to detect stars in images taken onboard a spacecraft, with its primary goal being to determine the spacecraft's attitude. It can also detect other bright objects, such as space debris and artificial objects, which reflect sunlight and Earth's albedo and appear in the detector images. From an image taken by the star tracker sensor, the star tracker will detect blobs, or bright regions, within the dark background. The centroiding algorithm determines the center of these blobs and passes this information to the star tracker algorithms. These algorithms use a database of known star positions to identify stars and then calculate the spacecraft's orientation, often described in the form of a quaternion.

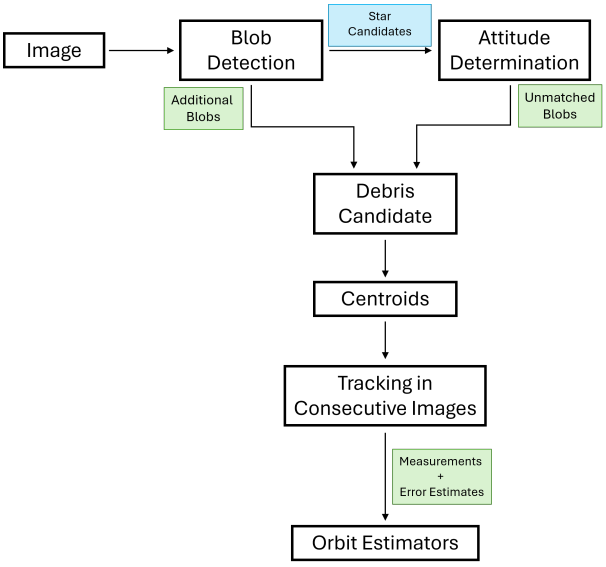

Figure 8: DeDUST debris tracking process.

Debris Detection Using Star Trackers (DeDUST) leverages the existing flow of star tracker algorithms. While most optical sensors process all blobs (bright regions) in an image to determine if they correspond to space debris, a star tracker can significantly reduce this workload by identifying many of these blobs as stars. The traditional star tracker algorithm flow is slightly adjusted for DeDUST. Figure 8 illustrates the DeDUST debris detection and tracking process.

Since stars are infinitely far away from the observer—in this case, the star tracker—their motion in the field of view depends solely on the spacecraft's angular rate. In contrast, space debris is much closer to the observer, so its motion and streak direction in the field of view depend on the relative angular velocity between the spacecraft and the debris. A preliminary categorization is performed based on the blob size and direction; stars will exhibit consistent behavior, while space debris may appear as outliers. Figure 9 illustrates the difference between debris streaks and star streaks. Unmatched blobs from the attitude determination algorithm are also selected as debris candidates.

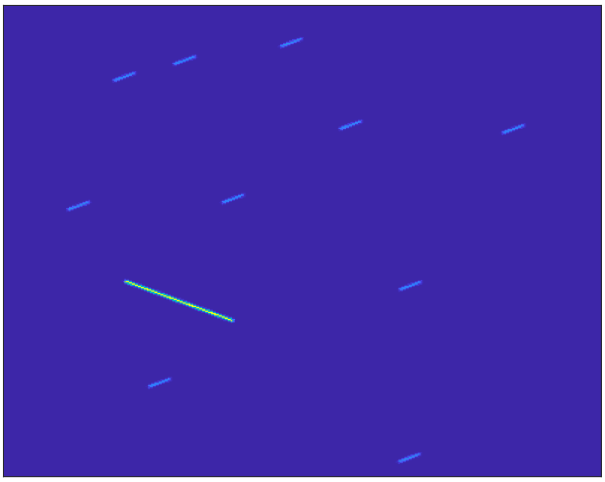

Figure 9: Debris streak among star streaks.

The number of blobs can be further reduced by analyzing subsequent images to verify if debris candidates are consistently present and display a trajectory consistent with space debris. By withholding only these remaining objects, the amount of data to downlink is significantly decreased.

Centroiding Kalman Filter

The centroid tracking algorithm in this work is based on the method proposed by Delabie.[8] Using a

first-order approximation Taylor expansion, the dynamic of star vectors can be written as:

$$\vec{s}_t = (I_{3x3} - \Delta T \omega_x)\vec{s}_{t-1} \tag{3}$$

Where $\vec{s}$ is the unit star vector, $\vec{\omega}$ is angular velocities and ΔT the exposure time. The star centroid as the function of the star vector $\vec{s}$, and focal length f is calculated by:

$$\begin{bmatrix} x_t \\ y_t \end{bmatrix} = f \begin{bmatrix} s_{y_t} \,/\, s_{x_t} \\ s_{z_t} \,/\, s_{x_t} \end{bmatrix} \tag{4}$$

Simplifying and expanding the expression in Equation 3 and substituting for elements in Equation 4, the expression for the star centroid model is obtained.

$$\begin{bmatrix} x_t \\ y_t \end{bmatrix} = \begin{bmatrix} 1 & -\Delta T\omega_x \\ \Delta T\omega_x & 1 \end{bmatrix} \begin{bmatrix} x_{t-1} \\ y_{t-1} \end{bmatrix} + f \begin{bmatrix} \Delta T\omega_z \\ \Delta T\omega_y \end{bmatrix} \tag{5}$$

Given the relationship in Equation 5 and the angular velocity measurement noise of σ_w, the propagated variance for the centroiding Kalman filter is:

$$\widetilde{P}_t = \begin{bmatrix} 1 & -\Delta T\omega_x \\ \Delta T\omega_x & 1 \end{bmatrix} \hat{P}_{t-1} \begin{bmatrix} 1 & -\Delta T\omega_x \\ \Delta T\omega_x & 1 \end{bmatrix}^T + \begin{bmatrix} 0 & f\Delta T & -y_t\Delta T \\ f\Delta T & 0 & x_t\Delta T \end{bmatrix} \begin{bmatrix} \sigma^2_{\omega_x} & 0 & 0 \\ 0 & \sigma^2_{\omega_y} & 0 \\ 0 & 0 & \sigma^2_{\omega_z} \end{bmatrix} \begin{bmatrix} 0 & f\Delta T & -y_t\Delta T \\ f\Delta T & 0 & x_t\Delta T \end{bmatrix}^T \tag{6}$$

The measurements in this study are blob centroids ($\widetilde{x}_t$, $\widetilde{y}_t$) from stars in the FOV and their are modeled in Kalman filter by:

$$\begin{bmatrix} x_t \\ y_t \end{bmatrix} = \underbrace{\begin{bmatrix} 1 & 0 \\ 0 & 1 \end{bmatrix}}_{H} \begin{bmatrix} \widetilde{x}_t \\ \widetilde{y}_t \end{bmatrix} \tag{7}$$

The Kalman gain K_t is calculated by:

$$K_t = \widetilde{P}_t H^T \left[H \widetilde{P}_t H^T + R \right]^{-1} \tag{8}$$

Where R is centroid stability errors from Figure 5. The detector response in the blob pixels is summed to obtain the total brightness and visual magnitude of the detected objects.

$$R = \begin{bmatrix} \sigma_x^2 & 0 \\ 0 & \sigma_y^2 \end{bmatrix} \tag{9}$$

The updated state and covariance matrix are then computed.

$$\begin{bmatrix} \hat{x}_t \\ \hat{y}_t \end{bmatrix} = \begin{bmatrix} x_t \\ y_t \end{bmatrix} + K_t \left(\begin{bmatrix} x_t \\ y_t \end{bmatrix} - H \begin{bmatrix} \widetilde{x}_t \\ \widetilde{y}_t \end{bmatrix} \right) \tag{10}$$

$$\hat{P}_t = (\mathbf{I} - K_t H)\, \widetilde{P}_t \, (\mathbf{I} - K_t H)^T + K_t R {K_t}^T \tag{11}$$

This work explores using a second Kalman filter for debris candidates, as their motion model differs from that of detected stars. The dynamic model is simplified by assuming linear motion within the FOV and it estimates the object's velocity from consecutive measurements. This assumption is valid for sensors with short exposure times and relatively low angular velocity conditions.

$$\begin{bmatrix} x_t \\ y_t \end{bmatrix} = \underbrace{\begin{bmatrix} 1 & 0 \\ 0 & 1 \end{bmatrix}}_{\Phi} \begin{bmatrix} x_{t-1} \\ y_{t-1} \end{bmatrix} + \begin{bmatrix} \Delta T v_x \\ \Delta T v_y \end{bmatrix} \tag{12}$$

$$v_t = \begin{bmatrix} (x_t - x_{t-1}) \,/\, \Delta T \\ (y_t - y_{t-1}) \,/\, \Delta T \end{bmatrix} \tag{13}$$

The single-time step blob velocity, v_t process noise as a function of centroid noise is written as:

$${\sigma_v}^2 = \Delta T^2 (\sigma_x^2 + \sigma_y^2) \tag{14}$$

To reduce the process noise and smooth the centroid velocities, this work uses a moving average of N number of past v_t measurements. The processing noise for the new velocity measurement, $\bar{v}_t$ could be propagated as

$${\sigma^2}_{\bar{v}} = \frac{{\sigma_v}^2}{N} \tag{15}$$

For the second approach, the propagated variance of Kalman filter is calculated by:

$$\widetilde{P}_t = \begin{bmatrix} 1 & 0 \\ 0 & 1 \end{bmatrix} \hat{P}_{t-1} \begin{bmatrix} 1 & 0 \\ 0 & 1 \end{bmatrix}^T + Q_k \tag{16}$$

where:

$$Q = \begin{bmatrix} \sigma_{vx}^2 & 0 \\ 0 & \sigma_{vy}^2 \end{bmatrix} \tag{17}$$

The remainder of the centroiding Kalman filter equations remain similar to the latter approach.

To utilize the estimated position of detected debris in orbit estimation algorithms, they are con-

verted to star tracker measurement vector by:

$$\vec{s_t} = \begin{bmatrix} s_x \\ s_y \\ s_z \end{bmatrix} = \begin{bmatrix} \frac{1}{\sqrt{1+\left(\frac{\hat{x}_t}{f}\right)^2+\left(\frac{\hat{y}_t}{f}\right)^2}} \\ \frac{\frac{-\hat{x}_t}{f}}{\sqrt{1+\left(\frac{\hat{x}_t}{f}\right)^2+\left(\frac{\hat{y}_t}{f}\right)^2}} \\ \frac{\frac{\hat{y}_t}{f}}{\sqrt{1+\left(\frac{\hat{x}_t}{f}\right)^2+\left(\frac{\hat{y}_t}{f}\right)^2}} \end{bmatrix} \tag{18}$$

The $\vec{s_t}$ measurements are rotated into the ECI frame using star tracker attitude solution A_t as:

$$\vec{b} = A_t \vec{s_t} \tag{19}$$

The observations right ascension α and declination δ is calculate from $\vec{b}$ by:

$$\alpha = \text{asin}\left(b_z\right) \tag{20}$$

and

$$\delta = \text{atan2}\left(b_y, b_x\right) \tag{21}$$

The right ascension and declination of the observations are passed onto orbit determination to characterize the space debris.

Orbit Determination Framework

Processed star tracker measurements are used to estimate the orbit of the observed object. Observations in the form of right ascension and declination are used within a batch least squares orbit determination algorithm in order to obtain a precise state corresponding to a given set of observations.

Physical Models

The process of orbit determination includes physical models to simulate the behaviour of the debris and the observations. The modelling can be divided into two parts: orbital dynamics and observations.

The precise orbit determination algorithm will aim to estimate a set of initial parameters of the debris element, i.e. the position and velocity of the element at the beginning of the observation arc. This initial state will be propagated for the duration of the observation arc using the orbital dynamics models. At any given observation epoch, the observation model will be used to simulate what an observation of the object at that epoch and propagated state would be. The estimation process then aims to minimize the difference between actual observations and simulated observations to determine the best guess for the initial state.

Orbital Dynamics

In order to accurately model the dynamics of an observed debris element, the following forces were taken into account:

- Earth gravitational model:
  - Spherical harmonics gravitational model with degree and order 8
- Aerodynamic drag:
  - Cannonball model for cross-sectional area and US76 density model
- Third-body gravitational perturbations:
  - Sun
  - Mars
  - Moon

The numerical integration of the equations of motion is done using a variable time-step Runge-Kutta-Fehlberg integrator of order 7 with error estimation of order 8 (RKF78).

Observation Model

The observation model for the angular measurement of an object is straightforward. If the position of the observer and the target are known as $\mathbf{r}_R$ and $\mathbf{r}_T$, the observable $\mathbf{h}_{ang.pos.} = [\alpha; \delta]$ can be calculated as follows:

$$\Delta\mathbf{r} = \mathbf{r}_R(t_R) - \mathbf{r}_T(t_T) \tag{22}$$

$$\tan\alpha = \frac{\Delta\mathbf{r}_y}{\Delta\mathbf{r}_x} \tag{23}$$

$$\delta = \frac{\Delta\mathbf{r}_z}{\sqrt{\Delta\mathbf{r}_x^2 + \Delta\mathbf{r}_y^2}} \tag{24}$$

Note the difference in time between $\mathbf{t}_R$ and $\mathbf{t}_T$, being caused by the time it takes for the light from the target to the receiver. This $\Delta t = \frac{||\Delta r||}{c}$, where c is the speed of sound. Now that both orbital dynamics and observation models are known, the estimation can be performed.

Orbit Estimation

Finally, once the observation modelling and the dynamics modelling are implemented, the estimation process can begin. For this, an initial guess is needed. For the initial guess, an angles-only Gauss method[9] is used, which determines an initial state for a set of 3 angular measurements. The further estimation process is shown in Figure 10. The batch least squares process is an iterative process wherein the observation residuals are minimized in order to create an updated initial state of the debris element.[10] After 10 iterations or after a residual threshold is crossed, the process is stopped and the solution is obtained.

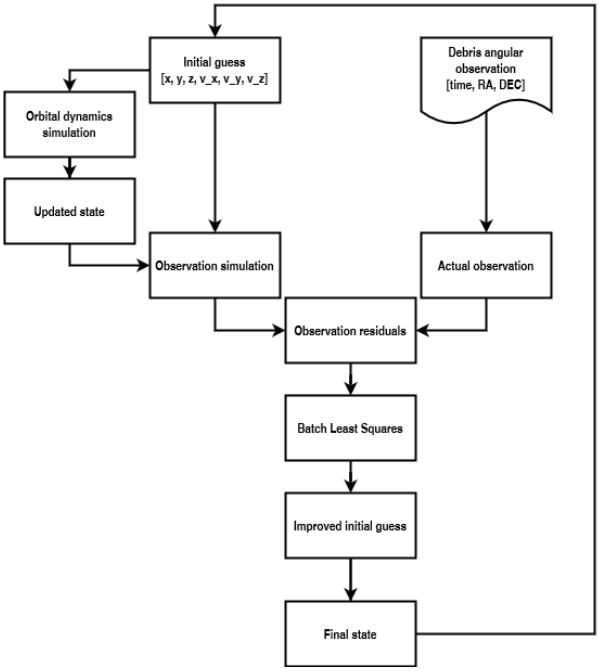

Figure 10: DeDUST orbit determination process.

Results and Discussions

The proposed approach is implemented and tested with a series of hardware-in-the-loop real night sky tests. First, all the bright blobs within the star tracker images are detected and after the matching step is completed, the unmatched blobs in two consecutive images are processed using the Hungarian algorithm[11] to find correspondence between the measurements. Removal of stars reduces the computational effort required by the debris tracking algorithm.

The matched stars are assigned automatically between the consecutive frames. The unmatched objects are processed by a Hungarian algorithm to find the best assignment for tracking. The velocity of matched stars on the FOV is calculated. For the unmatched objects, first, their velocity is computed and if this value is an outlier and higher compared to the star velocity, it is considered a debris candidate and tracked as long as it appears within the FOV.

Experimental Set up

Arcsec's star trackers have been placed on the Mercator telescope on La Palma. Figure 11 displays the hardware-in-the-loop test set up. Rapid night sky tests and software verifications can be performed using these facilities. Due to atmospheric aberration and weather conditions, detecting space debris will be more challenging on Earth. The purpose of the experiment was to test if nonstar objects can be detected and tracked in consecutive image frames.

Figure 11: Sagitta and Twinkle star tracker in La Palma.

Hardware-in-the-loop Night Sky Tests

Night sky tests were performed on arcsec's Sagitta star tracker placed on the Mercator telescope on La Palma. During the test, arcsec does not have control over the star tracker's pointing. The Sagitta star tracker is limited to tracking space debris appearing in its field of view opportunistically.

This section will present a sample instance of Sagitta star tracker detecting space debris on-ground. Figure 12 plots all the detected centroids by Sagitta star tracker during the night sky tests. The centroiding Kalman filter based on star tracker measurements was applied during the night sky trials to detect debris centroids from star centroids.

Figure 13 plots the detected centroids classified as stars or debris by Sagitta star trackers. The suggested algorithm employed on the detected centroids by Sagitta star tracker hardware in the loop tests, successfully classified space object instances from stars in the image.

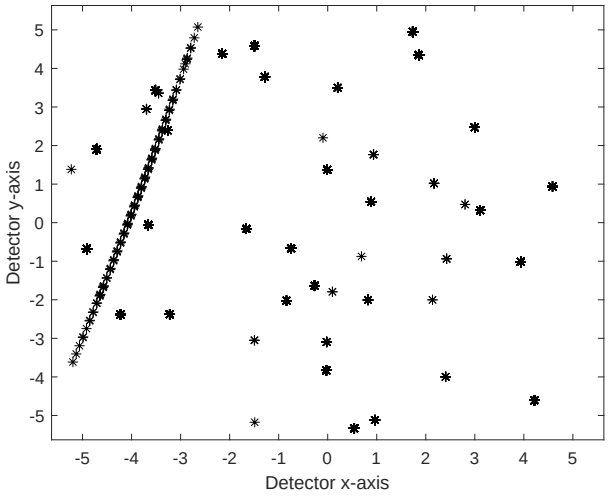

Figure 12: All detected centroids by Sagitta star tracker during night sky test.

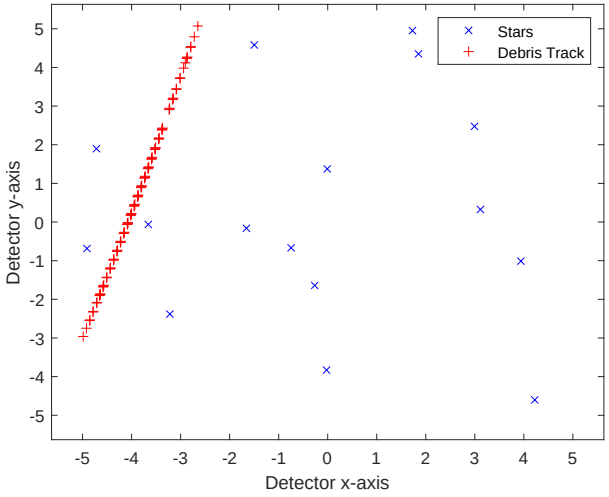

Figure 13: Sagitta star tracker classifying detected centroids into stars and debris categories.

Post Processing Orbit Determination

Based on the measurements from hardware-in-the-loop night sky tests, an initial and precise orbit determination was performed on the data from the night of April 30th 2024. The resulting orbit was plotted in STK and was then compared against a set of known bright objects. The resulting orbit and matched object is shown in Figures 14 and 15. The matched object was found to be the SUZAKU satellite, a joint JAXA and NASA astronomy satellite that has been defunct since 2015, making this observation a true demonstration of tracking space debris using star trackers.

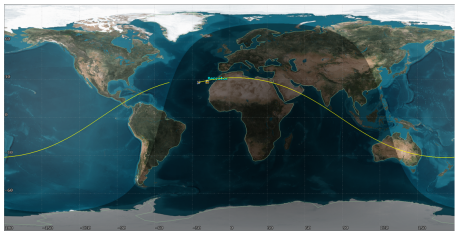

Figure 14: Ground track of orbit determination result (created with AGI STK).

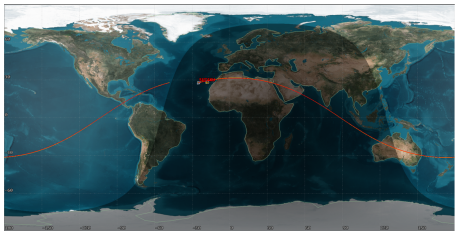

Figure 15: Ground track of matched object.

Conclusion and Future Work

This work investigated the concept of opportunistic detection of space debris using star trackers. The results serve as proof of concept for DeDUST using arcsec's Sagitta star tracker as the baseline sensor, but the presented work can be applied to other optical sensors. Simulation results demonstrated the possibility of detecting and tracking space debris within star tracker images and separating them from the detected stars.

The presented strategy is efficient since it employs star tracker baseline algorithms and detection strategies to reduce the computational burden of tracking space debris observations. The space debris data points can be integrated into already existing databases and applied for space traffic management or space debris cleanup efforts. The orbit determination process for angular measurements from star trackers was shown to work with the processed measurements. A set of nightsky observations was used to match the track to a known object and the functionality of both the centroiding Kalman filter and the orbit determination algorithms.

For future work, the star tracker measurement error covariance should be incorporated in orbit determination algorithms for more accurate characterization. The accuracy of the orbit determination will be increased in the future by implementing the following features in the orbit determination pipeline:

1. Timing bias correction

2. Covariance propagation
3. Satellite parameter estimation (area/mass ratio, ballistic coefficient, reflectivity)

Acknowledgments

The authors extend their gratitude to the EIC for generously funding the DeDUST project via the EIC Accelerator grant.

References

[1] Space Environment Statistics · Space Debris User Portal, May 2024. [Online; accessed 8. May 2024].

[2] Dario Spiller, Edoardo Magionami, Vincenzo Schiattarella, Fabio Curti, Claudia Facchinetti, Luigi Ansalone, and Alberto Tuozzi. On-orbit recognition of resident space objects by using star trackers. *Acta Astronautica*, 177:478–496, 2020.

[3] Meiying Liu, Hu Wang, Hongwei Yi, Yaoke Xue, Desheng Wen, Feng Wang, Yang Shen, and Yue Pan. Space debris detection and positioning technology based on multiple star trackers. *Applied Sciences*, 12(7):3593, 2022.

[4] Yasin Zamani, Joel Amert, Thomas Bryan, and Neda Nategh. A robust vision-based algorithm for detecting and classifying small orbital debris using on-board optical cameras. In *Advanced Maui Optical and Space Surveillance Technologies Conference*, number M19-7620, 2019.

[5] Troelz Denver, Mathias Benn, John L Jørgensen, Peter S Jørgensen, Matija Herceg, and Jack E Connerney. Space debris detection and tracking using star trackers. In *Geophysical Research Abstracts*, volume 21, 2019.

[6] Tjorven Delabie, Joris De Schutter, and Bart Vandenbussche. An accurate and efficient gaussian fit centroiding algorithm for star trackers. *The Journal of the Astronautical Sciences*, 61:60–84, 2014.

[7] Carl Christian Liebe. Accuracy performance of star trackers-a tutorial. *IEEE Transactions on aerospace and electronic systems*, 38(2):587–599, 2002.

[8] Tjorven Delabie. Star position estimation improvements for accurate star tracker attitude estimation. In *AIAA Guidance, Navigation, and Control Conference*, page 1332, 2015.

[9] D.A. Vallado. *Fundamentals of Astrodynamics and Applications*. Space technology library. Springer London, Limited, 2022.

[10] O. Montenbruck and E. Gill. *Satellite Orbits: Models, Methods, and Applications*. Physics and astronomy online library. Springer Berlin Heidelberg, 2000.

[11] Harold W Kuhn. The hungarian method for the assignment problem. *Naval research logistics quarterly*, 2(1-2):83–97, 1955.